SCIENTIFIC REPORTS

OPEN

SUBJECT AREAS:
ELECTRONIC MATERIALS
ELECTRONIC DEVICES

Received
29 November 2013

Accepted
7 April 2014

Published
24 April 2014

Correspondence and requests for materials should be addressed to H.W. (hwang@mail.xjtu.edu.cn) or C.-P.W. (cp.wong@mse.gatech.edu)

The use of polyimide-modified aluminum nitride fillers in AlN@PI/Epoxy composites with enhanced thermal conductivity for electronic encapsulation

Yongcun Zhou[1,2], Yagang Yao[2,3], Chia-Yun Chen[2], Kyoungsik Moon[2], Hong Wang[1] & Ching-ping Wong[2,4]

[1]Electronic Materials Research Laboratory, Key Laboratory of Ministry of Education & International Center for Dielectric Research, Xi'an Jiaotong University, Xi'an 710049, China, [2]School of Materials Science and Engineering, Georgia Institute of Technology, 771 Ferst Drive NW, Atlanta, GA 30332, United States, [3]Suzhou Institute of Nano-tech and Nano-bionics, Chinese Academy of Sciences, Suzhou 215123, China, [4]Department of Electronic Engineering, The Chinese University of Hong Kong, ShaTin, Hong Kong.

Polymer modified fillers in composites has attracted the attention of numerous researchers. These fillers are composed of core-shell structures that exhibit enhanced physical and chemical properties that are associated with shell surface control and encapsulated core materials. In this study, we have described an apt method to prepare polyimide (PI)-modified aluminum nitride (AlN) fillers, AlN@PI. These fillers are used for electronic encapsulation in high performance polymer composites. Compared with that of untreated AlN composite, these AlN@PI/epoxy composites exhibit better thermal and dielectric properties. At 40 wt% of filler loading, the highest thermal conductivity of AlN@PI/epoxy composite reached 2.03 W/mK. In this way, the thermal conductivity is approximately enhanced by 10.6 times than that of the used epoxy matrix. The experimental results exhibiting the thermal conductivity of AlN@PI/epoxy composites were in good agreement with the values calculated from the parallel conduction model. This research work describes an effective pathway that modifies the surface of fillers with polymer coating. Furthermore, this novel technique improves the thermal and dielectric properties of fillers and these can be used extensively for electronic packaging applications.

Surface modification of fillers in composites has recently received great attention due to as produced core-shell structures with unusually remarkable properties, such as large surface area, low density, and potential applications. The composites have myriad applications in controlled release, catalysis, and chemical storage[1–9]. These core-shell structures are gaining quite a lot of attention because they exhibit significant synthetic challenges. The resulting nanostructures exhibit enhanced physical and chemical properties owing to their shell surface control and encapsulated core materials. Ganguli's photocatalytic studies[10] have indicated that the ZnO/CdS core/shell nanorod arrays exhibit better degradation efficiency compared to bare ZnO and CdS under simulated solar radiation. The shell thickness also affected the photocatalytic efficiency that plays a pivotal role in the degradation of rhodamine B. The shell thickness of 30 nm CdS exhibited highest photocatalytic efficiency. Therefore, polymer composites made of core-shell structured fillers will have superior properties than bare core or shell based polymer composites. In recent times, several research studies have elucidated the controlled preparation of surface-modified fillers, such as metal@SiO_2[11–15], metal@metal[16,17], metal@carbon[18–21], metal@ploymer[22–25], etc. However, we need to devise newer methodologies to synthesize surface-modified fillers that can electronically encapsulate high performance polymer composites.

Aluminum nitride (AlN) has been extensively used as substrate material owing to its numerous attractive properties, such as high thermal conductivity, low thermal expansion coefficient, attractive dielectric properties, and excellent mechanical properties[26]. In polymer-based composites, AlN has been used to increase stiffness, reduce thermal expansion, and increase thermal conductivity of composites[26–31]. Gonsalves et al.[32,33] studied the preparation and properties of AlN-polyimide (PI) nanocomposite. According to these researchers, the thermal conductivity increased greatly when AlN was added to the PI matrix. At the same time, the coefficient of thermal expansion (CTE) also decreased significantly. However, several research studies have not elucidated the use of

polymer coating of AlN with well-defined core-shell structures. These are used for high performance electronic packaging of composite materials. In this research study, we developed a new method to coat a thin layer of PI on the surface of AlN particles. Thereafter, PI modified AlN particles were dispersed in epoxy resin. By adopting this approach, we could enhance the thermal and dielectric properties of the core-shell particle incorporated composite containing 10–40 weight percent of fillers. At 40 wt% of filler loading, the highest thermal conductivity of the PI-modified AlN composite reached 2.03 W/mK. This enhances the thermal conductivity by approximately 10.6 times than that of the epoxy matrix used. The experimental results of thermal conductivity were in good agreement with the calculated value from a parallel conduction model. This research study shows an effective pathway to modify the surface of fillers with polymer coating. Furthermore, the thermal and dielectric properties of these fillers can be enhanced with the adoption of this novel methodology and they can be extensively used for electronic packaging applications.

Results and Discussions

Figure 1a shows a schematic diagram that illustrates the preparation of PI modified AlN particles. Briefly, AlN surface was first functionalized by 3-mercaptopropionic acid (MPA) to avoid the agglomeration in ethanol. Thereafter, poly(amic acid) (PAA) modified AlN was synthesized using 3,3′,4,4′-benzophenonetetracarboxylic dianhydride (BTDA) and bis(4-aminophenyl) ether (ODA) monomers in dimethylacetamide (DMAc) solution. Finally, PI modified AlN was obtained after imidization of PAA modified AlN, which is referred as AlN@PI. Figures 1b and 1c illustrate the scanning electron microscopy (SEM) images of untreated AlN particles and AlN@PI, respectively. As shown in the Figure 1b, the diameter of pure AlN particles is approximately 1 μm. As shown in Figure 1c, PI is thoroughly coated on the surface of AlN particles after surface modification. In this case, the particles were attached to each other. The polymer shell seemed to form necking between particles. This necking could be beneficial for heat transfer in composites.

Figure 2 illustrates SEM images of AlN@PI/epoxy composites with different filler contents. The AlN@PI particles are homogenously distributed within the epoxy matrix. No obvious aggregation of the AlN@PI particles in the composite can be observed even with higher filler loading. High filler loadings (>35 vol%) are typically necessary to achieve an appropriate level of thermal conductivity in thermally conducive polymer composites, which leads to significant processing challenge. Moreover, a high inorganic filler loading also dramatically alters the mechanical behavior and density of polymers. At the same time, it increases the thermal conductivity of composites. Hence, we need to maintain a comparatively low level of filler loading in composites for ensuring good flowability.

The thermal conductivities of all composites greatly depend on the properties of polymers and fillers, such as their content, components, and the surface treatment of filler. The thermal conductivity and dielectric constant of all composites increase with the increase of the filler loading. Have to point out is that it is disfigurement such as air hole, impurity etc. in composites that is a very important factor to account the effective thermal conductivity of composites[34,35]. In Figure 3, we have compared the thermal conductivity of AlN@PI/epoxy and untreated AlN/epoxy composites containing 10–40 weight percent of fillers. An obvious increase in the thermal conductivity of composites is achieved by increasing the composition of filler loadings from 10% to 40%. The thermal conductivity values of AlN@PI/epoxy composites are larger than that of AlN/epoxy at every stage. In other words, it implies that untreated A1N particles are less effective than PI-modified AlN particles, which are used as fillers in composites to improve thermal conductivity in polymer composites. At 40 wt% of fillers loading, the highest thermal conductivity of the composite can reach 2.03 W/mK. At higher filler loading, the thermal conductivity of composites decreases due to voiding that is associated with imperfect filler packing and preparation technology[34]. So, we chose the 40% filler for performing this experiment. In this case, the composite material ensures excellent mechanical properties and processing performance.

Figures 3c and 3d illustrate the frequency dependency of relative permittivity and tan delta of AlN@PI/epoxy and AlN/epoxy compo-

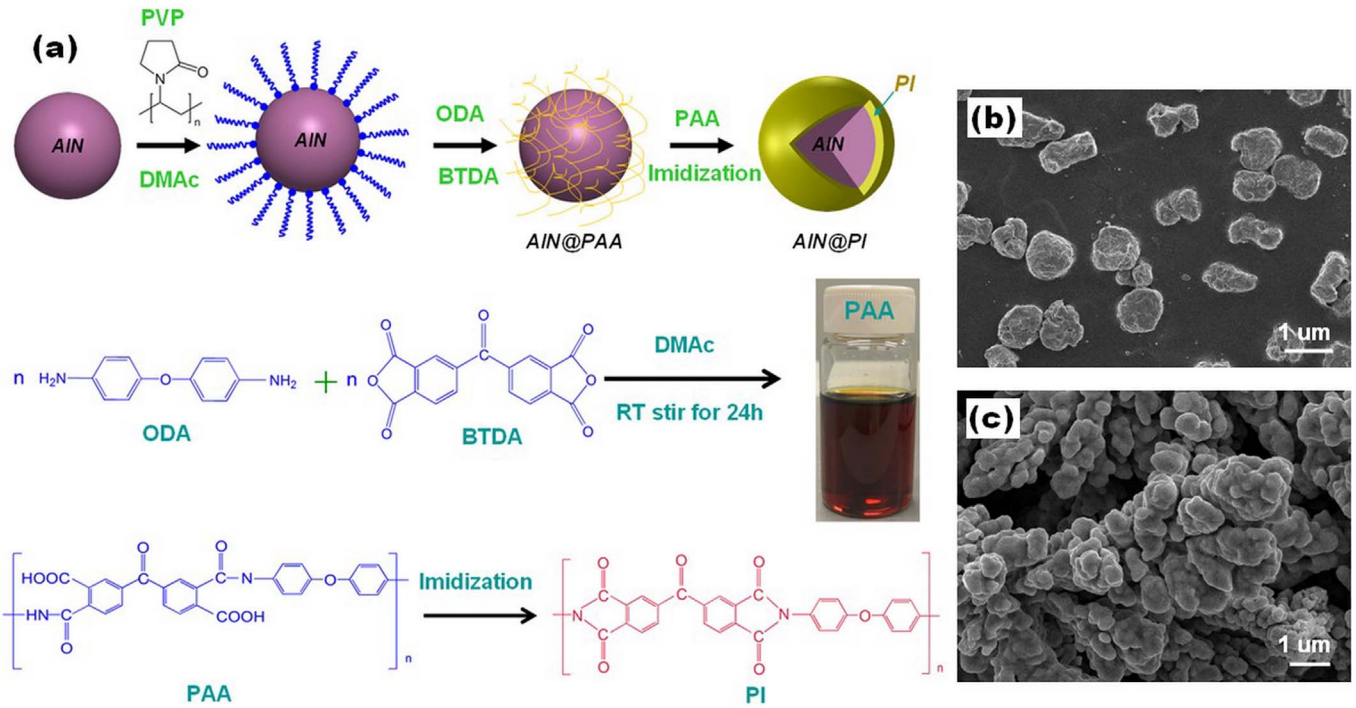

Figure 1 | (a) Schematic diagram depicting the formation process of AlN@PI particles. SEM images of (b) untreated AlN particles and (c) PI modified AlN particles.

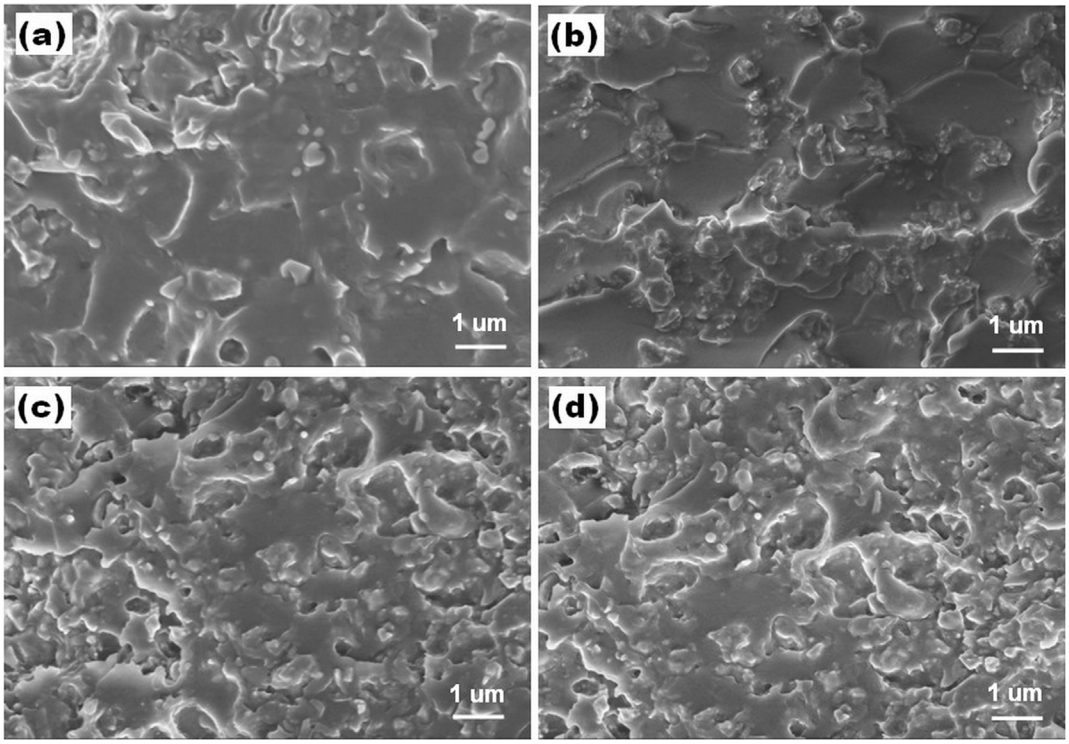

Figure 2 | SEM images of (a) 10 wt%, (b) 20 wt%, (c) 30 wt%, and (d) 40 wt% AlN@PI/epoxy composites having different filler loading.

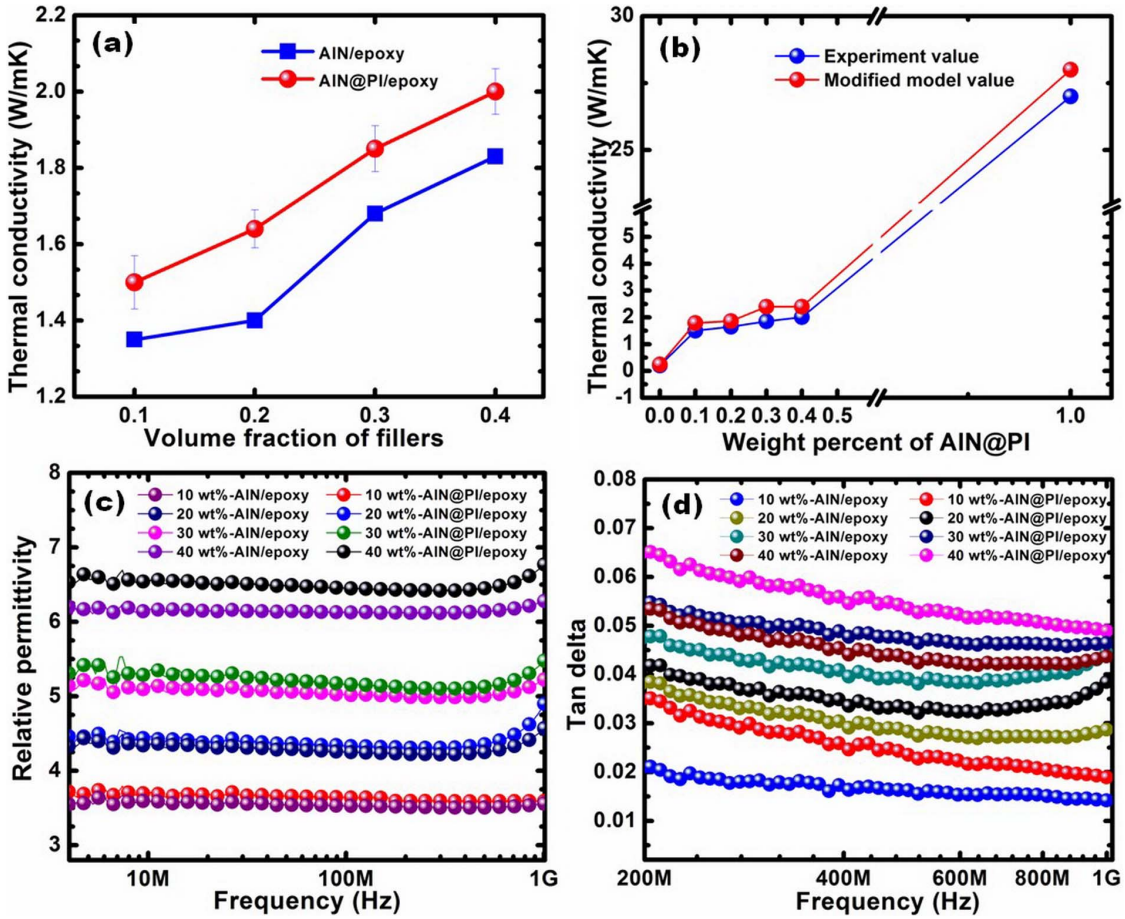

Figure 3 | (a) Thermal conductivity of AlN@PI/epoxy and untreated AlN/epoxy composites using 10–40 wt% of fillers. (b) Experimental results and modified model values of thermal conductivity as a function of filler loading of the AlN@PI/epoxy composites. The frequency dependency of (c) relative permittivity and (d) tan delta of the AlN@PI/epoxy and AlN/epoxy composites with different weight percent of fillers in frequency range (2 MHz–1 GHz).

Table 1 | Thermal conductivity and dielectric properties of various ceramic/polymer composites. v_f represents volume fraction

Materials	Filler loading	Thermal conductivity (W/mK)	Permittivity (1 MHz)	Year	Ref.
AlN/Polyimide	32 v_f	0.75	-	2004	[26]
AlN/LLDPE	70 wt	1.25	4.2	2011	[27]
AlN/PMMA	70 v_f	1.87	4.4	2012	[28]
AlN/Epoxy	36 v_f	1.46	-	2013	[29]
Al/Epoxy	0.48v_f	1.47	33	2010	[30]
GNPs/Epoxy	0.027wt	0.72	80	2013	[31]
AlN@PI/Epoxy	40 wt	2.03	6.85		our work

sites with different loading of fillers in the frequency range (2 MHz–1 GHz). Figure 3c illustrates a slight decrease in the permittivity of composites with an increase in frequency. At each filler loading, the relative permittivity of AlN@PI/epoxy composites is found to be larger than that of AlN/epoxy when the same frequency is maintained. All the relative permittivity curves versus frequency are nearly parallel to the frequency axis in the logarithmic scale. The relative permittivity of 40 wt% composite is 6.57 at 100 MHz. As shown in Figure 3d, all tan deltas of composites also hold a low level in the frequency range of 2 MHz–1 GHz. At a certain frequency, the tan delta decreases by increasing the concentrations of fillers, which is characterized with an increase in the porosity of the composite[36]. In general, PI possesses a low dielectric constant (~3.4 @1 MHz) and tan delta of a few parts per thousand, while it was coated on the AlN particles as a filler in composite, arising from the formation of bond bridge between organic and inorganic materials, that is, filler and polymer. Furthermore, the resulting tan delta is decreased significantly, thereby indicating that the extent of interfacial polarization is substantially augmented with a gradual reduction in frequency. In fact, interfacial polarization plays a crucial role in polymer composite materials, because additives, fillers, and even impurities have larger masses than the low molecular weight dipoles, making these systems heterogeneous. It is a well-known fact that both relative permittivity and tan delta depend on electronic, ionic, dipole-orientation, and space charge polarizations[26,37]. It is the porosity ratio, air volume fraction in composites that is also a very important factor to effect the thermal and dielectric properties of composites. The present system of composite is a triphase mixture of materials having different dielectric properties. It can be seen that composite possess a good compact and less porosity structure at 40% fillers from Fig. 2d SEM image. Therefore, we conclude that it can be attributed to not only the physicochemical characteristics of materials but also process conditions. Moreover, the composite with a distinct interphase between three phases illustrates an apparent loss at whole frequencies.

The thermal conductivity of AlN@PI/epoxy composites is greatly enhanced by adding PI-modified AlN particles that act as fillers. Table 1 provides a comparative overview of thermal conductivity and dielectric permittivity enhancement of AlN@PI/epoxy with reported ceramic/polymer composites. The thermal conductivity enhancement of AlN@PI/epoxy is the highest for low filler loading[26–31]. Table 1 also illustrates that filler modification is responsible for low filler loading. The thermal conductivity of AlN@PI/epoxy is enhanced by about 10.6 times than the pure epoxy. Moreover, the thermal conductivity of AlN@PI/epoxy is approximately 1.5–6 times higher than that from above-mentioned research works[26–31]. As shown in Figure 4a, the chemical structure of pure AlN, pure PI, and AlN@PI were investigated using Fourier Transform Infrared Spectroscopy (FTIR). There are three strong peaks near 3000 cm^{-1} which disappeared after reacting with PAA, thereby indicating that there exists a strong interaction between $-NH_2$ groups and AlN in the three spectrums. The results indicate that PI has yielded a large coverage on the surface of AlN particles by forming robust bindings. The bindings of PI to the surface of AlN particles are characterized by strong C-H stretching (2925 cm^{-1}) and C-N stretching (1435 cm^{-1}) absorptions, both of which are attributed to PI.

Figure 4b illustrates TGA results of 10–40 wt% of AlN@PI/epoxy composites under nitrogen atmosphere. The typical weight loss is observed at approximately 400°C. Due to the incomplete combustion of samples in nitrogen atmosphere, the eventual stable positions of all curves are higher than that of actual weight percentage. However, the chart illustrates the regularity and consistency of all samples. In addition, the composites show a high heat resistance to temperature at 250°C, which would be beneficial for electronic devices.

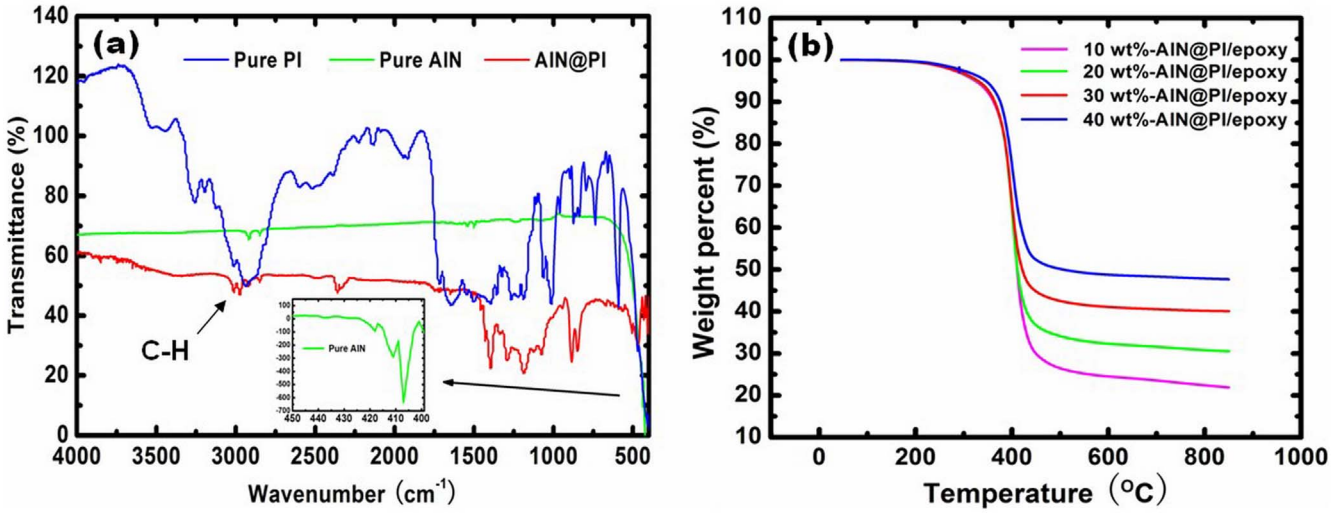

Figure 4 | (a) FTIR spectra of pure AlN, pure PI, and AlN@PI particles and (b) TGA profiles of 10–40 wt% of AlN@PI/epoxy composites under nitrogen atmosphere.

The effective thermal conductivity of a composite is strongly affected by its composition, structure, intrinsic thermal conductivity, filler particle size, shape, and interfacial thermal resistance, etc. The interfacial thermal resistance exerts a significant impact on the thermal conductivity of composite[38,39]. To elucidate the effective thermal conductivities of two-phase mixtures and polyphase mixtures of composites, several equations incorporating theoretical and empirical models have been developed[40–46]. Herein, we applied the modified parallel conduction model to calculate the thermal conductivity of AlN@PI/epoxy composites and compared it with our experimental data. The equations 1–3 were used to predict thermal conductivity values,

$$k_c = (1-\phi)\cdot k_m + \phi\cdot k_f \quad (1)$$

where, k represents thermal conductivity, c stands for composite, m stands for matrix, f stands for filler, and ϕ is the volume fraction of filler.

For series conduction model, the following equation is commonly used,

$$\frac{1}{k_c} = \frac{1-\phi}{k_m} + \frac{\phi}{k_f} \quad (2)$$

In this work, a similar conduction model is adopted,

$$\frac{1}{k_c} = \frac{\phi_1}{k_{f1}} + \frac{\phi_2}{k_{f2}} + \frac{\phi_m}{k_m} + \frac{\phi}{k_a} \quad (3)$$

where k_c, k_{f1}, k_{f2}, k_m, and k_a are the thermal conductivities of composite, AlN, PI, epoxy matrix, and air, respectively. ϕ_1, ϕ_2, ϕ_m, and ϕ are the content fractions of AlN, PI, epoxy matrix, and air in composites, respectively. The ϕ value can be obtained by correlating relative density with theoretical density.

In Figure 3b, we have compared the experimental and modified model values of thermal conductivity of the composites with different volume proportions of surface modified fillers. We found that the predicted thermal conductivity values of composites are in good agreement with the experimental results. Moreover, when the volume fraction of fillers increases, the corresponding thermal conductivity also increases gradually. In this model, several actual factors, such as disfigurement and impurity can be neglected for facilitating calculation. On the other hand, it was found that the porosity ratio (air volume fraction in composites) is an important factor that affects effective thermal conductivity in this conduction model, even though the content and density of air are much less than those of the fillers and PI matrix. The experimental results are lower than the simulation model values at all time.

In summary, we have presented homogeneous polymer composites comprising of surface modified AlN particles with an epoxy matrix. PI is used as the surface modification agent that is successfully coated on the surface of AlN particles. The results clearly illustrate that the polymer coating on AlN cores can significantly improve the thermal conductivity and dielectric properties of composites, whereas the dielectric losses are maintained at a relatively low level compared with that of uncoated AlN particles. The highest thermal conductivity of the composite can reach 2.03 W/mK at 40 wt% fillers loading. This shows that it exhibits 10.6 times of enhancement in thermal conductivity than that of epoxy matrix. The relative permittivity of 40 wt% composite is 6.57 at 100 MHz. In addition, the underlying mechanism of thermal conductivity was discussed systematically. The simulation thermal model was also proposed, thereby illustrating their agreement with experimental results. Our results indicate that the polymer coating is an effective surface modification method that is used to form core-shell structure, which can be used for fabricating ceramic-polymer composites of high thermal conductivity.

Methods

Materials. The monomers of BTDA and ODA of PI were supplied by Alfa Aesar Co. The solvent of DMAc (Sigma-Aldrich Company) and (3-Aminopropyl) triethoxysilane (APTS) (Sigma-Aldrich Company) were stirred using powdered calcium hydride overnight. Thereafter, this solvent was distilled under reduced pressure and stored over 4 Å molecular sieves, prior to use. AlN powder was supplied by Dow Chemical Co. The average diameter of AlN particles was about 1 μm at a loading of 3.26 g/cm^3. The specific surface area of AIN particles was greater than 75 m^2/g. The AlN powder was white in color and in the form of small agglomerates. All the monomers and AlN powder were dried in a vacuum oven at 120°C for 3–5 h prior to use. The epoxy resin is a mixture of diglycidyl ether of bispenol A and 3,4-epoxy cyclohexylmethyl-3,4-epoxy cyclohexyl carboxylate. Hexahydro-4- methyl phthalic anhydride and 1-cyanoethyl-2-ethyl-4- methylimidazole were used as curing agent and catalyst, respectively. Other chemicals and solvents were commercially obtained and used, as received. Table S1 illustrates the typical properties of aluminum nitride, BTDA/ODA polyimide, and epoxy resin.

Synthesis of PI precursor, BTDA-ODA PAA. PAA was synthesized using BTDA and ODA monomers with the same molar ratio, which was used to dissolve in DMAc solution. The reaction vessel consisted of a three-neck round-bottom flask equipped with nitrogen inlet, thermo-meter, and a condenser with a Dean-Stark trap. All monomers were added to a reaction vessel and were stirred at an ambient temperature until ODA and BTDA were dissolved completely. Then, the temperature of this solution was raised to 35°C. After attaining a temperature of 35°C, the process of stirring was continued for 24 h. As shown in Figure 1a, a viscous PAA solution was obtained.

Surface modification of AlN fillers. AlN powder (2 g) was dispersed in ethanol (500 ml) by gentle stirring and sonication. To avoid the agglomeration of AlN particles, MPA was used to functionalize AlN surface. Then, BTDA (1.5 g), ODA (2.48 g), and DMAc (15 ml) were added into the mixtures and a 1/1 molar ratio of BTDA/ODA was maintained. Subsequently, the mixtures were stirred with nitrogen inlet and a condenser for 24 h. Thereafter, the synthesized PAA was successfully coated on the surface of AlN particles. The solution was separated from the suspension by subjecting it to centrifugation at 5,000 rpm for 30 mins. Then, these obtained particles were step-dried at the following intervals: 80°C for 1 h, 120°C for 1 h, 200°C for 1 h, and 300°C for 1 h in a vacuum oven, respectively. Finally, we obtained polymer modified AlN powders with PI, referred as AlN@PI.

Preparation of AlN@PI-epoxy composites. The four different weight fractions (10–40) AlN@PI/epoxy composites were prepared by homogeneously mixing epoxy resins with surface modified AlN powder. This was done by performing sonication for 5 mins. In this process, a small amount of acetone was added to help the dispersion of AlN and then removed by a vacuum at elevated temperatures. Thereafter, the curing agent and catalyst were added and mixed by stirring. The composite was transferred to an aluminum foil mold and cured at 150°C for 2 h in a vacuum oven.

Characterizations. Transmission electron microscopy (TEM) was carried out using JEOL TEM 100CX. SEM (LEO 1530 and 1550) was used to characterize the morphology of AlN@PI/epoxy composite surfaces using an accelerating voltage of 3 kV, where the samples were sputter-coated with a thin layer of gold for better imaging. The dielectric properties of composites were be measured from 1 MHz to 3 GHz by RF impedance analyzers of E4991A (Agilent) with the 16453A dielectric material test fixture. Thermomechanical analyzer (TMA, Q-400 TA Instruments) was used to measure the CTE of composites. The thermal diffusivity (α) of AlN@PI/epoxy composites was measured using laser flash method with a LFA 447 (NETZSCH). The thermal conductivity was calculated by $\lambda = \alpha\rho C_p$, in which ρ and C_p are the density and heat capacity of AlN@PI/epoxy composites, respectively. The C_p was measured using differential scanning calorimetry (DSC, Q-600 TA Instruments). All thermal measurements were carried out at room temperature.

1. Li, C. R., Zhang, X. N. & Cao, Z. X. Triangular and fibonacci number patterns driven by stress on core/shell microstructures. *Science* **309**, 909–911 (2005).
2. Zhou, Y. C. *et al.* A poly(vinylidene fluoride) composite with added self-passivated microaluminum and nanoaluminum particles for enhanced thermal conductivity. *Appl Phys Lett* **98**, 182906 (2011).
3. Zhou, Y. C. *et al.* Enhanced high thermal conductivity and low permittivity of polyimide based composites by core-shell Ag@SiO_2 nanoparticle fillers. *Appl Phys Lett* **101**, 012903 (2012).
4. Heckel, J. C., Kisley, L. M., Mannion, J. M. & Chumanov, G. Synthesis and self-assembly of polymer and polymer-coated Ag nanoparticles by the reprecipitation of binary mixtures of polymers. *Langmuir* **25**, 9671–9676 (2009).
5. Lai, X. Y. *et al.* General synthesis and gas-sensing properties of multiple-shell metal oxide hollow microspheres. *Angew Chem Int Ed* **50**, 2738–2741 (2011).
6. Gai, S. *et al.* Synthesis of magnetic, up-conversion luminescent, and mesoporous core–shell-structured nanocomposites as drug carriers. *Adv Funct Mater* **20**, 1166–1172 (2010).
7. Zalich, M. A., Baranauskas, V. V., Riffle, J. S., Saunders, M. & Pierre, T. G. Structural and magnetic properties of oxidatively stable cobalt nanoparticles encapsulated in graphite shells. *Chem Mater* **18**, 2648–2655 (2006).

8. Lu, Y. *et al*. Hydrophilic Co@Au yolk/shell nanospheres: synthesis, assembly, and application to gene delivery. *Adv Mater* **22**, 1407–1411 (2010).
9. Graf, C., Vossen, D., Imhof, A. & Blaaderen, A. A general method to coat colloidal particles with silica. *Langmuir* **19**, 6693–6700 (2003).
10. Khanchandani, S., Kundu, S., Patra, A. & Ganguli, A. K. Shell thickness dependent photocatalytic properties of ZnO/CdS core-shell nanorods. *J Phys Chem C* **116**, 23653–23662 (2012).
11. Zhou, Y. C. & Wang, H. An Al@Al_2O_3@SiO_2/polyimide composite with multilayer coating structure fillers based on self-passivated aluminum cores. *Appl Phys Lett* **102**, 132901 (2013).
12. Zhou, Y. C., Bai, Y. Y., Yu, K., Kang, Y. & Wang, H. Excellent thermal conductivity and dielectric properties of polyimide composites filled with silica coated self-passivated aluminum fibers and nanoparticles. *Appl Phys Lett* **102**, 252903 (2013).
13. Ung, T., Liz-Marzan, L. M. & Mulvaney, P. Controlled method for silica coating of silver colloids. Influence of coating on the rate of chemical reactions. *Langmuir* **14**, 3740–3748 (1998).
14. Gong, J. L., Jiang, J. H., Liang, Y., Shen, G. L. & Yu, R. Q. Synthesis and characterization of surface-enhanced Raman scattering tags with Ag/SiO2 core-shell nanostructures using reverse micelle technology. *J Colloid Interf Sci* **298**, 752–756 (2006).
15. Shanthil, M., Thomas, R., Swathi, R. S. & Thomas, K. G. Ag@SiO_2 core-shell nanostructures: distance-dependent plasmon coupling and SERS investigation. *J Phys Chem Lett* **3**, 1459–1464 (2012).
16. Liang, A. H., Liang, Y. Y., Jiang, Z. L. & Jiang, H. S. Resonance scattering spectral detection of catalase activity using Au@Ag nanoparticle as probe and coupling catalase catalytic reaction with fenton reaction. *J Fluoresc* **19**, 1009–1015 (2009).
17. Liu, F. K., Tsai, M. H., Hsu, Y. C. & Chu, T. C. Analytical separation of Au/Ag core/shell nanoparticles by capillary electrophoresis. *J Chromatogr A* **1133**, 340–346 (2006).
18. Su, X. C., Gutierrez, A., Yacaman, M. J., Dong, X. L. & Jin, S. Investigations on magnetic properties and structure for carbon-encapsulated nanoparticles of Fe, Co, Ni. *Mater Sci Eng A* **286**, 157–160 (2000).
19. Nishijo, J., Okabe, C., Oishi, O. & Nishi, N. Synthesis, structures andmagnetic properties of carbon-encapsulated nanoparticlesvia thermal decomposition of metal acetylide. *Carbon* **44**, 2943–2949 (2006).
20. Yu, D. S., Nagelli, E., Du, F. & Dai, L. M. Metal-free carbon nanomaterials become more active than metal catalysts and last longer. *J Phys Chem Lett* **1**, 2165–2173 (2010).
21. Sun, X. & Li, Y. D. Ag@C core/shell structured nanoparticles: controlled synthesis, characterization, and assembly. *Langmuir* **21**, 6019–6024 (2005).
22. Grass, R. N., Athanassiou, E. K. & Stark, W. J. Covalently functionalized cobalt nanoparticles as a platform for magnetic separations in organic synthesis. *Angew Chem Int Ed* **46**, 4909–4912 (2007).
23. Corr, S. A., Rakovich, Y. P. & Gun'ko, Y. K. Multifunctional magnetic-fluorescent nanocomposites for biomedical applications. *Nanoscale Res Lett* **3**, 87–104 (2008).
24. Decher, G. F. Nanoassemblies: toward layered polymeric multicompositesi. *Science* **277**, 1232–1237 (1997).
25. Donath, E., Sukhorukov, G. B., Caruso, F., Davis, S. A. & Mohwald, H. Novel hollow polymer shells by colloid-templated assembly of polyelectrolytes. *Angew Chem Int Ed* **37**, 2201–2205 (1998).
26. Xie, S. H., Zhu, B. K., Li, J. B., Wei, X. Z. & Xu, Z. K. Preparation and properties of polyimide/aluminum nitride composites. *Polym Test* **23**, 797–801 (2004).
27. Zhou, W. Thermal and dielectric properties of the AlN particles reinforced linear low-density polyethylene composites. *Therm Acta* **512**, 183–188 (2011).
28. Zhou, Y. C. *et al*. Fabrication and characterization of aluminum nitride polymer matrix composites with high thermal conductivity and low dielectric constant for electronic packaging. *Mater Sci Eng B* **177**, 892–896 (2012).
29. Zhu, B. L. *et al*. Preparation and properties of aluminum nitride-filled epoxy composites: Effect of filler characteristics and composite processing conditions. *J Appl Polym Sci* **127**, 3456–3466 (2013).
30. Zhou, W. & Yu, D. Thermal and dielectric properties of the aluminum particle/epoxy resin composites. *J Appl Polym Sci* **118**, 3156–3166 (2010).
31. Min, C., Yu, D., Cao, J., Wang, G. & Feng, L. A graphite nanoplatelet/epoxy composite with high dielectric constant and high thermal conductivity. *Carbon* **55**, 116–25 (2013).
32. Gonsalves, K. E., Chen, X. & Baraton, M. I. Mechanistic investigation of the preparation of polymer/ceramic nanocomposites. *Nanostru Mater* **9**, 181–184 (1997).
33. Chen, X., Gonsalves, K. E., Chow, G. M. & Xiao, T. D. Homogeneous dispersion of nanostructured aluminum nitride in a polyimide matrix. *Adv Mater* **6**, 481–484 (1994).
34. Wong, C. P. & Bollampally, R. S. Thermal conductivity, elastic modulus, and coefficient of thermal expansion of polymer composites filled with ceramic particles for electronic packaging. *J Appl Polym Sci* **74**, 3396–403 (1999).
35. Shimazaki, Y., Hojo, F. & Takezawa, Y. Preparation and characterization of thermoconductive polymer nanocomposite with branched alumina nanofiber. *Appl Phys Lett* **92**, 133309 (2008).
36. Li, Y. *et al*. Large dielectric constant and high thermal conductivity in poly (vinylidene fluoride)/barium titanate/Silicon Carbide three-phase nanocomposites. *ACS Appl Mater & Interfaces* **3**, 4396–403 (2011).
37. Yu, S., Hing, P. & Hu, X. Dielectric properties of polystyrene aluminum-nitride composites. *J Appl Phys* **88**, 398–404 (2000).
38. Zhao, X. H., Wu, Y. G., Fan, Z. G. & Li, F. Three-dimensional simulations of the complex dielectric properties of random composites by finite element method. *J Appl Phys* **95**, 8110 (2004).
39. Li, C. C., Fu, L. J., Jing, O. Y. & Yang, H. M. Enhanced performance and interfacial investigation of mineral-based composite phase change materials for thermal energy storage. *Sci Rep* **3**, 1908 (2013).
40. Zhou, S. X. *et al*. Experiments and modeling of thermal conductivity of flake graphite/polymer composites affected by adding carbon-based nano-fillers. *Carbon* **57**, 452–459 (2013).
41. Hauser, R. A., Keith, J. M., King, J. A. & Holdren, J. L. Thermal conductivity models for single and multiple filler carbon/liquid crystal polymer composites. *J Appl Polym Sci* **110**, 2914–2923 (2008).
42. Usowicz, B., Lipiec, J., Usowicz, J. B. & Marczewski, W. Effects of aggregate size on soil thermal conductivity: Comparison of measured and model-predicted data. *Int J Heat Mass Tran* **57**, 536–541 (2013).
43. Sitprasert, C., Dechaumphai, P. & Juntasaro, V. A thermal conductivity model for nanofluids including effect of the temperature-dependent interfacial layer. *J Nanopart Res* **11**, 1465–1476 (2009).
44. Seo, B. H. *et al*. Model for thermal conductivities in spun yarn carbon fabric composites. *Polym Compos* **26**, 791–798 (2005).
45. Clancy, T. & Gates, T. Modeling of interfacial modification effects on thermal conductivity of carbon nanotube composites. *Polymer* **47**, 5990–5996 (2006).
46. Liu, Y., Zhang, Z. Y., Wei, X. L., Li, Q. & Peng, L. M. Simultaneous electrical and thermoelectric parameter retrieval via two terminal current-voltage measurements on individual ZnO nanowires. *Adv Funct Mater* **21**, 3900–3906 (2011).

Acknowledgments

The authors acknowledge funding support from the Natural National Science Foundation of China (61025002 and 51372265), and the China Scholarship Council (201206280056).

Author contributions

Z.-Y.C. contributed to the conception and design of the experiment, analysis of the data and writing the manuscript with assistance of Y.-Y.G., C.-C.Y. and M.-K. W.-H. and W.-C.P. modified the final version of the manuscript. All authors discussed the results and commented on the manuscript.

Additional information

Supplementary information accompanies this paper at http://www.nature.com/scientificreports

Competing financial interests: The authors declare no competing financial interests.

How to cite this article: Zhou, Y.C. *et al*. The use of polyimide-modified aluminum nitride fillers in AlN@PI/Epoxy composites with enhanced thermal conductivity for electronic encapsulation. *Sci. Rep.* **4**, 4779; DOI:10.1038/srep04779 (2014).